The Mechanochemistry of Molecular Motors

David Keller* and Carlos Bustamante†‡

*Department of Chemistry, University of New Mexico, Albuquerque, New Mexico 87131; and †Departments of Physics and Cellular and Molecular Biology, University of California, Berkeley, California 94720 USA, ‡Physical Biosciences Division, Lawrence Berkeley National Laboratory, Berkeley, California 94720, USA

ABSTRACT A theory of molecular motors is presented that explains how the energy released in single chemical reactions can generate mechanical motion and force. In the simplest case the fluctuating movements of a motor enzyme are well described by a diffusion process on a two-dimensional potential energy surface, where one dimension is a chemical reaction coordinate and the other is the spatial displacement of the motor. The coupling between chemistry and motion results from the shape of the surface, and motor velocities and forces result from diffusion currents on this surface. This microscopic description is shown to possess an equivalent kinetic mechanism in which the rate constants depend on externally applied forces. By using this equivalence we explore the characteristic properties of several broad classes of motor mechanisms and give general expressions for motor velocity versus load force for any member of each class. We show that in some cases simple plots of 1/velocity vs. 1/concentration can distinguish between classes of motor mechanisms and may be used to determine the step at which movement occurs.

INTRODUCTION

Molecular motors are single protein molecules that convert chemical energy, usually in the form of adenosine triphosphate (ATP) into mechanical forces and motion. Most organisms have many different motors that are specialized for particular purposes such as cell division, cell crawling, maintaining cell shape, movements of internal organelles, etc. A large number of biological motors and motorlike proteins have been discovered and characterized in recent years. (Spudich, 1994), and there is considerable variation in design and behavior among them, ranging from the two-headed "hand-over-hand" motion of the kinesins and the "rowing" motion of the myosins, to the crawling of DNA and RNA polymerases, to the proton-powered rotary motions of bacterial flagellar motors and F_1F_o ATP synthases. Despite this diversity, several lines of evidence suggest that many such "mechanochemical" proteins, which use chemical energy to carry out mechanical processes, share fundamental underlying features that can be understood with the same basic concepts and theories.

Together with the discovery of new motorlike systems, a growing body of experimental results has been accumulating, particularly from experiments carried out on single or few motor molecules (Kuo and Sheetz, 1993; Svoboda et al., 1993; Finer et al., 1994; Yin et al., 1995; Coppin et al., 1996, 1997; Higuchi et al., 1997; Hua et al., 1997; Mehta et al., 1997; Schnitzer and Block, 1997; Vugmeyster et al., 1998). The variables most naturally and accurately measured in such single-molecule experiments are force, distance, and time. These are also the variables of greatest functional significance for molecular motors. The availability of distance, force, and velocity as direct experimental observables is beginning to provide a body of basic facts on which well-founded theories of molecular motor function can be built. Recent theoretical efforts have produced both detailed models for specific motor molecules (Derenyi and Vicsek, 1996, 1998; Guajardo and Sosa, 1997; Elston et al., 1998; Julicher and Bruinsma, 1998; Wang et al., 1998a), and investigations of the basic physics of mechanochemical systems (Magnasco, 1993, 1994; Millonas and Dyckman, 1994; Millonas, 1995; Astumian and Bier, 1994; Astumian, 1997; Julicher et al., 1997). A common theme is that motor proteins may generate forces and vectorial motion by rectifying thermal fluctuations. In such "fluctuation ratchet" models, chemical energy does not produce force directly. Rather, the motor diffuses along its track (or some other position coordinate) by random walk, and the chemical reaction merely biases the walk so that steps in the forward direction are more probable than backward steps.

We begin by outlining the general principles by which the theory of stochastic process is applied to molecular motors. The motor molecule is thought of as a small machine operating in a thermal bath, subjected to large fluctuations in conformation and chemical state. These microscopic fluctuations all but disappear in the long-term and large-number ensemble averages involved in bulk experiments, but are direct observables in experiments involving few or single molecules. This physical picture of the motor as a microscopic fluctuating machine corresponds to a random walk or diffusion process on the potential energy surface of the system. The diffusion fluxes that result from this random walk yield both rates of chemical reaction and mechanical velocities for the motor.

This leads to a simple but general theory by which any molecular motor or molecular machine can be modeled. We derive well-founded general expressions for kinetic rate constants that depend on external force, which can then be incorporated into kinetic schemes to predict mechanochemical properties. The stochastic theory thus makes the connec-

Received for publication 26 April 1999 and in final form 27 October 1999.

Address reprint requests to Dr. Carlos Bustamante, Dept. of Physics, 173 Birge Hall, University of California, Berkeley, CA 94720. Tel.: 510-643-9706; Fax: 510-642-5943; E-mail: carlos@alice.berkeley.edu.

0006-3495/00/02/541/16 $2.00

tion between the microscopic view in which protein conformational changes, external forces, and thermal fluctuations are explicitly accounted for, and the macroscopic and phenomenological view of chemical kinetics. As examples of the theory, we investigate four simple classes of molecular motors, and explore the generic behavior within each class.

MOLECULAR MOTORS AS STOCHASTIC MACHINES

A molecular motor is an enzyme (or in some cases a complex between an enzyme and a track such as actin or DNA) that generates force and motion. The ensemble average behavior of a motor can be described phenomenologically by standard chemical kinetics if rates of reaction are related to the rates of physical motion, and if rate constants vary with external force in a known way. Thus, on the macroscopic scale a molecular motor is seemingly simple and well-behaved. However, if it were possible to follow in atomic detail the actual events that take place in a single motor protein, a very different view would emerge. On the microscopic scale the motor protein is more naturally described as a small mechanical device driven through a cyclic series of conformational states by a combination of rapid chemical events (such as binding of small "fuel" molecules, bond-breaking processes, and unbinding processes), and incessant, rapid thermal fluctuations. In many cases thermal fluctuations are an essential component of the molecular mechanism of the motor/enzyme. For example, the ability of proteins to catalyze chemical reactions depends on thermally induced crossing of potential energy barriers, and the ability of molecular motors to generate forces may depend on thermally driven diffusion from one site on a filament (such as actin, DNA, or a microtubule) to the next. More importantly, it is at the level of such microscopic fluctuations that the connection between "chemical" quantities, such as free energies of reaction and kinetic rate constants, and "mechanical" quantities such as forces and velocities, is most naturally made. It is the purpose of this paper to outline the connection between these two views, in part to justify and give a microscopic interpretation to the macroscopic, phenomenological view, and in part to show how the microscopic view can be used to make detailed predictions regarding molecular motor mechanisms.

System and bath variables

On the microscopic scale a motor molecule (and its track, if any) is a small machine that can change conformation. All conformations can be described by a set of conformational variables, x_1, x_2, x_3, etc., which should rigorously include all the degrees of freedom (atom positions, bond angles, bond distances, etc.) of the molecule or molecules that make up the motor; but such a detailed description is obviously neither practical nor desirable in most cases. In the examples below we will assume that the most important motions of the molecule can be described with just a few parameters, which will be called system variables. As will be seen below, the system variables describe motions that are not at equilibrium on the time scale of the experimental observations. They are usually large, concerted protein movements such as the opening of a binding cleft, a change of molecular shape, binding or unbinding of a motor domain to a polymer track, or a movement of the protein along the track. They may also be smaller movements that are important to chemical reactions, such as the stretching and breaking of chemical bonds. Some variables may, like normal coordinates, describe more than one simultaneous motion.

Proteins contain many degrees of freedom, so the system variables do not describe most of the possible motions of the protein. As long as the "extra" motions are rapid, so that they are approximately at equilibrium on the time scale of the experiment, their effects can be accounted for as part of the background of equilibrium fluctuations that are always present. The extra degrees of freedom in both the protein and the surrounding solvent will therefore be referred to as bath variables. The bath variables do not appear explicitly in any of the equations or results of the stochastic theory. Their effects on the system variables are accounted for indirectly, as fluctuating stochastic forces or as contributors to potentials of mean force and to frictional forces.

Following Magnasco (1994) and Astumian and Bier (1994) we divide the system variables into two classes, corresponding to orthogonal axes in the conformational space of the motor. Because a molecular motor must have a source of chemical energy, at least one of the system variables must be a measure of progress of the chemical reaction, and will be called the chemical variable. All others will be called mechanical variables. If the chemical reaction cannot be described by a single coordinate, more chemical variables can be added without fundamentally changing the theory. For motors powered by energy sources other than a chemical reaction (for example, a proton gradient), the chemical variables can be redefined appropriately. The operative property is that progress along a chemical axis is accompanied by a chemical change (with its associated change in thermodynamic free energy), but does not involve net movement of the motor as a whole.

Of the mechanical variables, at least one must give the position of the motor. For motors such as myosin, kinesin, and RNA polymerase, the position variable is the location of the motor protein along its track (microtubule, actin filament, or DNA double helix, respectively). For rotary motors, such as the bacterial flagellar motor or the F_1F_o ATP synthase, the position variable is the rotational angle. As with the chemical variable, extra position variables can be added as needed to describe systems that are more complex. The distinguishing characteristic in this case is that motion along a position variable can be unbounded; that is, the motor can move as far as it likes. For the purposes of this paper we will designate x_1 as the chemical variable and x_2

as the position variable. Then $x_3, \ldots, x_n$ are mechanical variables that describe internal motions within the motor protein. By definition, motion along these "internal" variables is bounded.

State space of a motor molecule and the potential of mean force

The system variables define an n-dimensional state space for the motor, $x_1, \ldots, x_n$. Each point in the state space represents a unique conformation of the motor molecule. Associated with each conformation $x_1, x_2, \ldots, x_n$ is a free energy, $V(x_1, x_2, \ldots, x_n)$, called the potential of mean force (McQuarrie, 1976). It has the property that its derivatives with respect to $x_1, \ldots, x_n$ are the (time or ensemble) average forces, $\langle F_i \rangle$, along those variables:

$$\langle F_i \rangle = -\left(\frac{\partial V(x_1, \ldots, x_n)}{\partial x_i}\right)_{x_j \neq x_i}, \quad \text{all system variables } x_i \tag{1}$$

The potential of mean force can in principle be calculated (in the canonical ensemble) by integrating the Boltzmann factor, $\exp[-U(x_1, x_2, \ldots, x_n, y_1, y_2, \ldots, y_m)/kT]$, over the bath variables, $y_1, y_2, \ldots, y_m$, holding the system variables constant:

$$V(x_1, \ldots, x_n) = -kT \ln\left\{\int\int \cdots \int \exp\left(\frac{-U(x_1, x_2, \ldots, x_n, y_1, y_2, \ldots, y_m)}{kT}\right) dy_1 dy_2 \cdots dy_m\right\} \tag{2}$$

where $U(x_1, x_2, \ldots, x_n, y_1, y_2, \ldots, y_m)$ is the full potential for all degrees of freedom in the system, including protein, solvent, and other solution variables. Both entropic and enthalpic contributions to the free energy are included in the potential of mean force, so both entropic and mechanical forces are accounted for. Because the potential of mean force is an equilibrium quantity, all bath variables (which do not appear in V) are implicitly assumed to be at equilibrium.

For the simplest case, where the motor is described by only two system variables, the potential of mean force, $V(x_1, x_2)$, defines a two-dimensional potential energy surface on which the molecular motor moves (see Fig. 1). Along a line parallel to x_1, the chemical variable, this surface will look like a typical reaction free energy diagram, with local minima representing stable species separated by free energy barriers that determine the probability of transitions among the minima, and hence determine the rates of chemical reactions. After each chemical turnover the enzyme must return to its initial state, and the free energy must have decreased by a fixed amount (closely related to the macroscopic free energy for the chemical reaction). Therefore, the free energy surface is periodic in the chemical variable except for a linear term that accounts for the free energy of reaction. Along a line parallel to x_2, the position variable, the surface gives the local free energy changes associated with movement of the motor along its track. Inasmuch as the track is periodic, the potential must also be periodic, and in the absence of external forces the overall free energy change in one full step along the track, d, is zero. For example, for kinesin/tubulin, x_2 would be the position of kinesin along a microtubule, and the free energy surface along x_2 may have a periodic series of minima representing the stable binding sites for kinesin on the microtubule. Altogether, the poten-

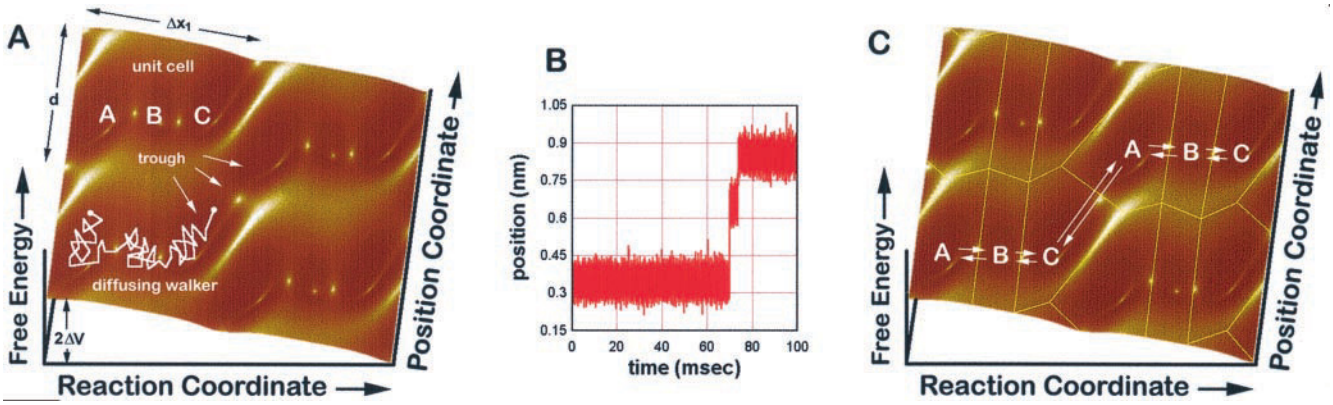

FIGURE 1 (*A*) Hypothetical potential energy surface (potential of mean force) for a simple motor with two system variables. The surface is periodic, with four unit cells shown. The trajectory in the lower right shows the path of a hypothetical system point executing a random walk on the surface. (*B*) Simulated run of position versus time data, calculated using the Langevin equations (Eqs. (4)) for a two-dimensional system with the potential surface in (*A*). (*C*) Kinetic scheme overlaid on the potential energy surface in (*A*). The fine lines show the boundaries of the regions corresponding to each macroscopic intermediate species. Each macroscopic species is identified with a minimum of the potential, and transitions between species are associated with low energy pathways between minima.

tial must satisfy (Magnasco, 1994)

$$\begin{aligned} V(x_1 + \Delta x_1, x_2, \ldots) &= V(x_1, x_2, \ldots) + \Delta V \\ V(x_1, x_2 + d, \ldots) &= V(x_1, x_2, \ldots), \end{aligned} \tag{3}$$

where ΔV is a constant, Δx_1 is the period along x_1, and d is the period along x_2 (i.e., the step size for the motor).

In a molecular motor the mechanical and chemical variables must be coupled in some way so that progress along the chemical reaction leads to movement. The nature of this coupling is contained in the contours of $V(x_1, x_2, \ldots, x_n)$ (see below). Therefore, all the important features of a molecular motor are determined by the potential of mean force, and the choice of $V(x_1, x_2, \ldots, x_n)$ defines the mechanism and properties of the motor (see below).

Stochastic equations of motion for a motor

So far there is nothing specifically microscopic in our description of a molecular motor. The chemical and mechanical operation of the motor is described by a potential energy function V, and the movements of the motor are movements of a point on an n-dimensional potential energy surface. On the macroscopic scale this motion would be governed by classical equations of motion, which would predict smooth trajectories through the molecule's conformation space. On the microscopic scale, however, the interaction of the system with the bath variables, representing the solvent and all degrees of freedom not explicitly accounted for in the system variables, is important. At a given temperature, T, each of the bath variables has energy of the order of kT. For a microscopic motor this energy is significant compared to the features of the potential energy surface, and is usually much larger than the kinetic energy associated with the system variables. The bath variables may therefore have large effects on the motion of the system variables, but it is assumed that these effects are random in a sense to be defined below.

This physical picture is well described by a system of classical Langevin equations (Kubo et al., 1995; Chandrasekhar, 1943),

$$\begin{aligned} \gamma_1 \dot{x}_1 &= -\frac{\partial V}{\partial x_1} + F_1(t) + \delta F_1(t) \\ \gamma_2 \dot{x}_2 &= -\frac{\partial V}{\partial x_2} + F_2(t) + \delta F_2(t) \\ &\vdots \\ \gamma_n \dot{x}_n &= -\frac{\partial V}{\partial x_n} + F_n(t) + \delta F_n(t) \end{aligned} \tag{4}$$

where $\gamma_1, \gamma_2, \ldots, \gamma_n$ are damping constants, $\delta F_1, \delta F_2, \ldots, \delta F_n$ are random bath forces, and $F_1(t)$, $F_2(t)$, etc. are external forces which may include, for example, a load force opposing the motion of the motor. These external forces may depend on time but are assumed not to depend on the system variables.

The classical inertial forces, $m_i \ddot{x}_i$, have been neglected in Eq. 4, which means that all motions are overdamped, and there are no oscillations or other "reactive" effects. This is a good approximation for the relatively slow time scale of much of the experimental data on molecular motors. Only very fast motions (vibrations of parts of the motor molecules with frequencies of a megahertz or higher) show significant inertial behavior in proteins, and these are averaged out on the slow time scale of the experimental measurements (from 0.1 ms to seconds or minutes). The damping terms, $\gamma_i \dot{x}_i$, are simple frictions, and do not allow for any "memory" (forces caused by reaction of the bath at a later time due to motions in x at an earlier time) on the experimental time scale. The effects of the bath variables appear in three ways in Eq. 4: in the damping terms on the left-hand side, $\gamma_i \dot{x}_i$; in the stochastic forces on the right hand-side, δF_1, δF_2; etc.; and in the potential of mean force, V. The stochastic forces are defined to have zero mean (any force that does not average to zero is included in the "external" forces F_1, F_2, etc):

$$\langle \delta F_i(t) \rangle = 0, \quad \text{all } i \tag{5}$$

In addition, the fact that the damping terms are written as simple frictions requires that the stochastic forces have δ-function time correlation (Mori, 1965; Kubo et al., 1995):

$$\begin{aligned} \langle \delta F_i(t) \delta F_i(t + \tau) \rangle &= 2\gamma_i kT \delta(\tau) \\ \langle \delta F_i(t) \delta F_j(t + \tau) \rangle &= 0, \quad i \neq j \end{aligned} \tag{6}$$

The δ-function in Eqs. 6 means that a force fluctuation at time t is completely uncorrelated with another force fluctuation an infinitesimal time later. The value of the force at any one time is taken to have a Gaussian distribution. This is consistent with a physical situation in which the actual forces are much faster than the time between experimental observations, so the apparent force is the sum of many small impulses. Notice also that Eqs. 6 do not depend on the absolute time t, but only on the time difference, τ. Thus, as would be expected for a bath at equilibrium, the statistical properties of the bath forces depend only on time intervals and not on the absolute value of time. Finally, the bath forces acting on different variables i and j are uncorrelated at all times.

Further insight into the nature of the stochastic forces is provided by the spectral density of fluctuations, which is just the Fourier transform of the correlation function:

$$\begin{aligned} \langle |\delta F_i(\omega)|^2 \rangle &= \int_{-\infty}^{\infty} \langle \delta F_i(t) \delta F_i(t + \tau) \rangle e^{i\omega t} dt \\ &= 2\gamma_i kT \end{aligned} \tag{7}$$

According to the right-hand side of Eq. 7, the intensity of fluctuations for δ-function correlated forces is independent of frequency, and hence is often called white noise.

Both of the approximations above—neglect of inertial forces and δ-function correlation of the stochastic forces—can be relaxed if necessary (Mori, 1965); but doing so greatly complicates both the mathematics and the interpretation of the results. In the absence of any experimental evidence that these complications are needed, we adopt the simpler theory.

The Smoluchowski equation

Equations 4–6 correspond to a system moving on a potential energy surface $V(x_1, x_2, \ldots, x_n)$, subjected to white noise of intensity $2\gamma_i kT$ at all frequencies. The presence of random forces causes the trajectory of the system point, $[x_1(t), x_2(t), \ldots, x_n(t)]$ to be random as well. Individual trajectories therefore have little significance by themselves. The important quantities are those that describe the statistics of many trajectories, and the proper solution to the Langevin equation (Eq. 4) is a probability distribution of trajectories.

The approximations made in the previous section—the fact that the bath forces lose all correlation after an infinitesimal time, and the neglect of inertial forces so that the equations of motion (Eq. 4) are first-order in time—mean that the system loses all memory of previous positions after each step. The motion of $x_1(t)$, $x_2(t)$, etc. is therefore a Markov walk or diffusion process (Kubo et al., 1995), described by a probability density, $w(x_1, x_2, \ldots, x_n; t)$, for observing the walker at location $x_1, x_2, \ldots, x_n$ at time t, given that it had distribution $w_o(x_1, x_2, \ldots, x_n)$ at the initial time, t_o. Because probability is conserved, w must obey a continuity equation:

$$\frac{\partial w}{\partial t} + \nabla \cdot J = \frac{\partial w}{\partial t} + \sum_{i=1}^{n} \frac{\partial J_i}{\partial x_i} = 0 \qquad (8)$$

where $\nabla = (\partial/\partial x_1, \partial/\partial x_2, \ldots, \partial/\partial x_n)$ is an n-dimensional gradient, and $J = (J_1, J_2, \ldots, J_n)$ is the n-component probability current density. For an n-dimensional biased diffusion process the current density is:

$$J_i = -\frac{kT\partial w}{\gamma_i \partial x_i} + \frac{f_i}{\gamma_i} w \qquad (9)$$

where f_i is the force acting along the ith dimension of the state space due both to the potential and external forces, but not the stochastic force:

$$f_i = -\frac{\partial V}{\partial x_i} + F_i(t) \qquad (10)$$

The first term in Eq. 9 is a diffusion current with diffusion constant $D_i = kT/\gamma_i$, in accordance with the Einstein relation between D and γ. The second term is a drift current due to forces acting on the random walker. The sign of the external force, $F_i(t)$, is chosen so that a positive force gives rise to a positive contribution to the current, J_i. In the molecular motor field it is conventional to express measured quantities in terms of load force, which is effectively the negative of F_i as written in Eqs. 9 and 10. We adhere to general usage for the sign of the force in the present section, but will switch to the molecular motor convention in the next and subsequent sections, where the application is more specifically to molecular motors.

Substituting Eqs. 9 and 10 into Eq. 8 yields the Smoluchowski equation:

$$\frac{\partial w}{\partial t} + \sum_{i=1}^{n}\left(-\frac{kT}{\gamma_i}\frac{\partial^2 w}{\partial x_i^2} + \frac{1}{\gamma_i}\frac{\partial}{\partial x_i}(f_i w)\right) = 0 \qquad (11)$$

In the one-dimensional case this reduces to

$$\frac{\partial w}{\partial t} - \frac{kT}{\gamma}\frac{\partial^2 w}{\partial x^2} + \frac{1}{\gamma}\frac{\partial}{\partial x}\left[\left(-\frac{\partial V}{\partial x} + F(t)\right)w\right] = 0 \qquad (12)$$

The Smoluchowski equation is a second-order partial differential equation that can be solved for $w(x_1, x_2, \ldots, x_n; t)$ at any time t, given a known distribution, w_o, at the initial time t_o. Once w is known, J can be found from Eq. 9.

Physical interpretation of the stochastic theory for molecular motors

Equations 8–12 govern all the behavior of a molecular motor, including its chemical kinetics, the average force and velocity generated by the motor, and the fluctuations about these mean values. The function $w(x_1, x_2, \ldots, x_n; t)$ is the probability that the motor will be found in the conformation given by $x_1, x_2, \ldots, x_n$ at time t, and contains all information on both the average motion of the molecular motor, and on its statistical fluctuations.

Consider the hypothetical potential energy surface for a molecular motor, $V(x_1, x_2)$, shown in Fig. 1 *A*. The motor has only two degrees of freedom (one chemical variable and one mechanical variable), so the free energy surface is also two-dimensional. According to the stochastic theory, the operation of a single motor during a single cycle is a random walk on this surface. The surface shown in Fig. 1 *A* is periodic along the chemical axis (except for a uniform tilt) and along the position axis, as is required for periodic chemical turnovers and periodic movement. For clarity, we have constructed a case where the distances between features along the chemical axis are similar to those along the mechanical axis, but the scales may be very different in real motors. For example, the movements involved in chemical bond breaking are usually on the angstrom scale, while motor stepping movements can be several nanometers.

Four unit cells are shown, each of which contains three potential energy minima (labeled A, B, and C in the unit cell in the upper right). Each minimum can be reached from the neighboring minima by low-energy "passes" between them. Together these passes define a low-energy path through the conformational space of the motor. The low-energy path, in turn, defines the most probable sequence of conformational changes as the motor goes through one mechanochemical cycle. During a cycle the diffusing system point will tend to stay near the minima of the deep wells, but will occasionally make transitions between wells through the passes. Hence the wells correspond to the stable states that would be found in kinetics experiments, and the low-energy passes between the wells define the reaction coordinates for transitions between kinetic intermediates.

The entire surface has a uniform tilt along the chemical axis. The drop in energy in one unit cell is the constant energy, ΔV, in Eq. 3. The tilt represents the thermodynamic driving force for the chemical reaction, and biases the diffusion process toward the products of the chemical reaction and away from reactants. At a given instant of time the system point may step in any direction, but over many steps the system will, on average, drift in the direction of the tilt.

The long trough in the center of Fig. 1 *A* is the crucial region where chemistry is coupled to mechanical motion. As long as the low-energy path is parallel to the chemical variable (as it is for transitions between the three closely spaced wells) no net change in position takes place. Experimentally, the motor would be seen to fluctuate about a fixed location on its track while purely chemical processes take place; but in the trough region the tilt of the potential in the chemical direction drives movement along the mechanical direction, and chemical energy is transduced into mechanical motion.

Fig. 1 *B* is a run of simulated single molecule data (motor position versus time) for a motor with the potential surface in Fig. 1 *A.* The simulation was carried out by numerically integrating the Langevin equations (Eq. 4) for the chemical and position variables, x_1 and x_2, with V given by the surface in Fig. 1 *A,* zero external forces, $F_i(t)$, and a stochastic force, $\delta F_i(t)$, given by Eqs. 5 and 6. Only the intrinsic fluctuations of the system itself are shown; no attempt has been made to add the instrumental noise present in experimental data. While the motor goes through the purely chemical part of its cycle, its position fluctuates rapidly, but the average velocity is zero. As the system enters the trough region a rapid stepping motion is observed with a large positive velocity. A second, smaller step occurs as the system falls from the left-hand well (labeled A in Fig. 1 *C*) to the lower well (C in Fig. 1 *C*). After these steps the average position again becomes constant and the average velocity drops to zero. Though this is a purely hypothetical example, the qualitative behavior—rapid steps separated by relatively long pauses—is similar to that observed in real motors (for examples see Coppin et al., 1996, 1997; Hua et al., 1997; Schnitzer and Block, 1997).

Connection to chemical kinetics: first-order rate constants

From the discussion above it is clear that the detailed, mechanical view that comes naturally from the stochastic theory is closely related to the simpler view that comes from chemical kinetics. Fig. 1 *C* shows the potential energy surface in Fig. 1 *A* overlaid with a kinetic scheme. Each potential well is identified with a kinetic intermediate, and the population, p_i, of each intermediate is the integral of the probability density $w(x_1, x_2)$ over the zone surrounding the corresponding well: $p_i = \int_{\text{zone i}} w(x_1, x_2)dx_1dx_2$, etc. The kinetic scheme is thus a "coarse-grained" version of the stochastic picture. In place of a continuous diffusion process, we now have transitions among discrete states A–C. In place of the continuous probability density, $w(x_1, x_2)$, we now have a set of discrete populations p_A, p_B, p_C; and in place of the continuous current density, $J(x_1, x_2)$, we have discrete currents (rates of reaction) dp_A/dt, dp_B/dt, dp_C/dt. The potential energy surface thus determines the kinetic mechanism for the motor. Conversely, knowledge of the kinetic mechanism gives information about the main features of the potential.

It is therefore possible to use a mixture of stochastic theory and kinetic information (from experiments) to build a detailed model for any molecular motor. In particular, the stochastic formalism can be used to calculate the rate constants for each kinetic transition. The calculated rate constants depend on the shape of the potential energy surface and on externally applied forces. Thus, the stochastic theory makes it possible to find rate constants as functions of external force, F.

Consider a single first-order chemical process, say, between species C and species A through the trough in the middle of Fig. 1 *C.* In the region between C and A the potential energy surface is shaped like a mountain pass (i.e., a saddle point), with negative curvature along the minimum energy path and positive curvature in the orthogonal direction. The boundary between A and C is defined to go through the saddle point at the top of the pass. Let s be the distance along the minimum energy path between C and A, and let t be a variable perpendicular to s at all points. If the transitions between C and A are slow compared to the diffusion time within the well, the system point will wander up and down the walls of the pass as it approaches the saddle point. It is then reasonable to make the approximation that the system is at equilibrium with respect to movements along t (perpendicular to the minimum energy path), and the nonequilibrium dynamics are accounted for by movements along s alone. The potential of mean force can then be redefined in the neighborhood of the pass by averaging over t:

$$e^{-V(s)/kT} = \int e^{-V(s,t)/kT} dt,$$

where $V(s, t)$ is the potential of mean force for the full two-dimensional surface, and $V(s)$ is the new, one-dimen-

sional potential of mean force for movements only along s. The variable s now plays the role of a one-dimensional reaction coordinate that involves concerted changes in both the chemical state of the motor and the physical position of the motor. Thus, for local transitions along the path from C to A, the problem has been reduced from two dimensions to one. As long as equilibrium is rapid along t, $V(s)$ still (implicitly) accounts for the effects of two dimensions. Effectively, t has been included in the bath variables.

The kinetic rate constants for a one-dimensional, first-order transition between any two species,

$$\mathrm{A} \underset{\mathrm{k_f}}{\overset{\mathrm{k_r}}{\leftrightarrows}} \mathrm{B},$$

can readily be found from the Smoluchowski equation (see above). Consider a steady-state process for which all quantities, including the currents and probability densities, are constant in time. Let $s = 0$ at the leading edge of the region corresponding to A, $s = \ell$ at the boundary between the A and B regions, and $s = L$ at the far edge of region B. For a one-dimensional system at steady state, the current density, J, must be constant in s, so from Eq. 9 we have

$$J = \text{const.} = -\frac{kT}{\gamma}\frac{dw}{ds} - \frac{1}{\gamma}\left(\frac{dV}{ds} + F\right)w \tag{13}$$

where F is an external load force along the local reaction coordinate, s. The form of Eq. 13 assumes that the motor molecule is rigid enough so that force components along directions other than s have no significant effect on the kinetics. The sign of F has been chosen opposite to the usual convention for force (and also opposite to the convention used in Eqs. 4–12), but is in keeping with the usual definition of force in the molecular motor field, where a positive (load) force opposes the movement of the motor, and hence contributes negatively to J.

Solving for $w(s)$ we obtain

$$w(s) = -e^{-(\mathrm{V(s)+Fs})/\mathrm{kT}}\left[\int_0^s e^{(\mathrm{V(s')+Fs})/\mathrm{kT}}ds'\,\frac{J\gamma}{kT} - e^{\mathrm{V(0)/kT}}w(0)\right] \tag{14}$$

Now we require that the integral of $w(s)$ over the A region equal the population of the (biochemical) state A, p_A, and the integral over the B region equal the population of state B, p_B:

$$\int_0^\ell w(s)ds = p_\mathrm{A}, \quad \int_\ell^\mathrm{L} w(s)ds = p_\mathrm{B} \tag{15}$$

Taking the integral of Eq. 14 over regions A and B yields a set of two linear equations that can be solved for J as a function of p_A and p_B:

$$\begin{aligned} p_\mathrm{A} &= -\frac{J\gamma}{kT}\Sigma_\mathrm{A} + N_\mathrm{A}w(0) \\ p_\mathrm{B} &= -\frac{J\gamma}{kT}\Sigma_\mathrm{B} + N_\mathrm{B}w(0), \end{aligned} \tag{16}$$

where

$$\begin{aligned} N_\mathrm{A} &= \int_0^\ell e^{-(\mathrm{V(s)-V(0)+Fs})/\mathrm{kT}}ds, \quad N_\mathrm{B} = \int_\ell^L e^{-(\mathrm{V(s)-V(0)+Fs})/\mathrm{kT}}ds \\ \Sigma_\mathrm{A} &= \int_0^\ell e^{-(\mathrm{V(s)+Fs})/\mathrm{kT}}\sigma(s)ds, \quad \Sigma_\mathrm{B} = \int_\ell^\mathrm{L} e^{-(\mathrm{V(s)+Fs})/\mathrm{kT}}\sigma(s)ds, \end{aligned} \tag{17}$$

and

$$\sigma(s) = \int_0^s e^{(\mathrm{V(s')+Fs})/\mathrm{kT}}ds'. \tag{18}$$

Solving for J yields

$$J = \left(\frac{kT}{\gamma}\frac{N_\mathrm{B}}{N_\mathrm{A}\Sigma_\mathrm{B} - N_\mathrm{B}\Sigma_\mathrm{A}}\right)p_\mathrm{A} - \left(\frac{kT}{\gamma}\frac{N_\mathrm{A}}{N_\mathrm{A}\Sigma_\mathrm{B} - N_\mathrm{B}\Sigma_\mathrm{A}}\right)p_\mathrm{B} \tag{19}$$

Comparing this to the form expected for a first-order reaction at steady state, $J = k_\mathrm{f}p_\mathrm{A} - k_\mathrm{r}p_\mathrm{B}$, gives the desired expressions for the forward and reverse rate constants as functions of load force:

$$\begin{aligned} k_\mathrm{f}(F) &= \frac{kT}{\gamma}\frac{N_\mathrm{B}}{N_\mathrm{A}\Sigma_\mathrm{B} - N_\mathrm{B}\Sigma_\mathrm{A}}, \\ k_\mathrm{r}(F) &= \frac{kT}{\gamma}\frac{N_\mathrm{A}}{N_\mathrm{A}\Sigma_\mathrm{B} - N_\mathrm{B}\Sigma_\mathrm{A}} \end{aligned} \tag{20}$$

Fig. 2 *b* gives examples of how $k_\mathrm{f}(F)$ and $k_\mathrm{r}(F)$ vary with force for a simple piecewise-linear potential that has two wells separated by a barrier. The potential is of the type shown in Fig. 2 *a,* but with symmetric wells ($\Delta s_\mathrm{f} = \Delta s_\mathrm{r} = \Delta s = 2.5$ nm, $L = 2\ell = 10$ nm, $\Delta V_0 = 0$, $\Delta V^\ddagger = V(L) = 12.5$ kJ/mol). When the applied force is large and negative, the forward rate constant is approximately linear in force: $k \propto (F_\mathrm{c} - F)/\gamma$, where γ is the damping constant and F_c is a constant offset force. Likewise, at large positive forces the reverse rate constant is approximately linear. This limit arises when the drift velocity alone dominates the transition rate, and both the potential energy barrier and back diffusion are unimportant.

When the applied force is positive, the forward rate constant, $k_\mathrm{f}(F)$, appears approximately exponential, consistent with the Arrhenius form, $k \propto \exp[(\Delta G^\ddagger - F\Delta s)/kT]$, where $\Delta G^\ddagger$ is an activation free energy and Δs is a charac-

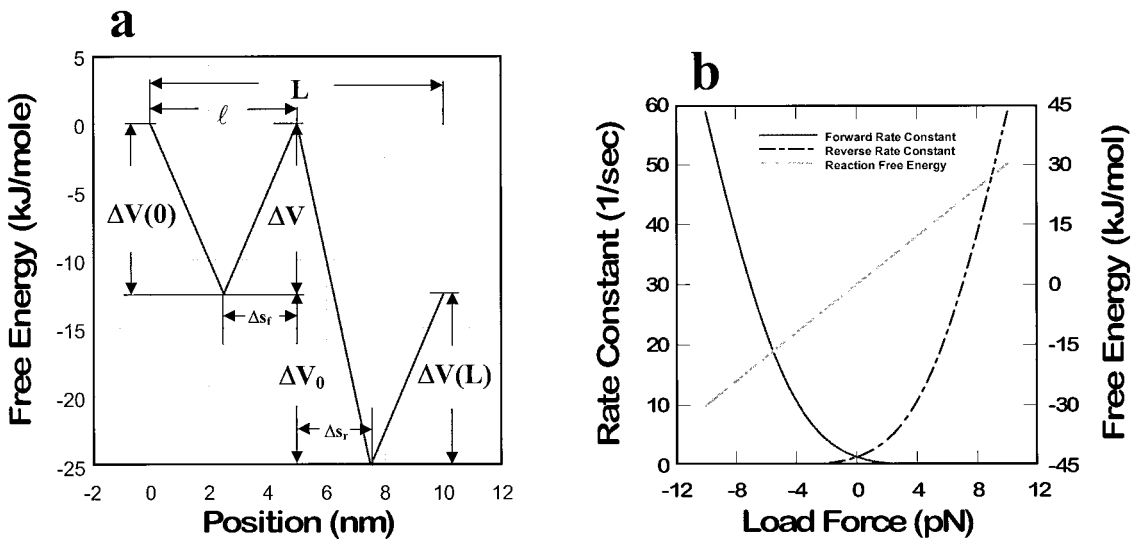

FIGURE 2 (*a*) Piecewise linear potential energy function with two wells separated by a potential energy barrier. The potential is defined by eight parameters ($\Delta V(0)$, ΔV, ΔV_0, $\Delta V(L)$, Δs_f, Δs_r, ℓ, and L) as shown in the figure. (*b*) Forward and reverse rate constants and reaction free energy as functions of load force. The curves were calculated from a potential of the type shown in (*a*) with $\Delta V(0) = \Delta V_0 = \Delta V(L) = 0$, $\Delta V = 12.5$ kJ/mol, $\Delta s_f = \Delta s_r = 2.5$ nm, $x = 5$ nm, $L = 10$ nm. The forward (reverse) rate constant is linear at large negative (positive) loads. The free energy is proportional to the natural log of the ratio of the forward and reverse rate constants. In the case shown the free energy is linear even in regions where one or both of the rate constants is nonexponential.

teristic length. Similarly, the reverse rate constant appears approximately exponential at negative forces. Because it is simple and familiar, the Arrhenius form is commonly used in molecular motor theories (Wang et al., 1998a, b). The activation free energy, $\Delta G^{\ddagger}$, is usually interpreted as a barrier height and Δs is interpreted as a step size for the motor. However, log plots of many calculations like the one in Fig. 2 *b* show that the rate constants are not exponential in force. In particular, a fit of the rate constants to an exponential function yields different values of $\Delta G^{\ddagger}$ and Δs from one range of forces to another. The Arrhenius form is thus useful as a generic fitting function over a limited range of forces, but the values of $\Delta G^{\ddagger}$ and Δs should be interpreted with caution.

For a potential with two wells separated by a barrier, as in Fig. 2 *a,* the rate constants are most sensitive to the distances from the well bottoms to the barrier top (Δs_f and Δs_r), the size of each well (ℓ and $L - \ell$), the barrier height (or activation energy, ΔV), and the energy difference between wells (ΔV_0). Once these parameters are specified, the detailed shape of the potential has relatively little effect.

Second-order rate constants

The results above apply only for first-order processes, but many models for molecular motors and molecular machines will include second-order steps that are affected by external force. For example, consider a motor for which movement and binding of a fuel molecule occur on the same step:

$$M + T \underset{k_1(F)}{\overset{k_{-1}(F)}{\rightleftarrows}} MT \qquad \text{mechanochemical binding}$$

where M is the motor molecule, T is the fuel molecule, and $k_1(F)$ and $k_{-1}(F)$ are force-dependent rate constants. The fact that the rate constants depend on force implies that the binding step involves net motion. Part of the binding energy is therefore converted into mechanical work.

Every binding process must involve at least two parts: a purely second-order process in which two molecules come into loose contact by diffusion alone, and a first-order process in which the two molecules undergo conformational changes that result in a more strongly bound state. We therefore divide the single step above into an equivalent two-step process:

$$M + T \underset{k_D}{\overset{k_{-D}}{\rightleftarrows}} M'T \underset{k_1(F)}{\overset{k'_{-1}(F)}{\rightleftarrows}} MT$$

where $M'T$ is a short-lived, loosely bound intermediate. The rate constants for the first step, k_D and k_{-D}, are assumed to be large compared to k'_1 and k'_{-1}, so $M'T$ is approximately at equilibrium with the free species M and T. Assuming that the diffusion process is not affected by external force (i.e., that external force acts on the protein but not on the fuel molecule directly), only k'_1 and k'_{-1} are force-dependent. Therefore $(M'T) \cong (k_D/k_{-D})(M)(T)$ and the effective rate

constants for mechanochemical binding, k_1 and k_{-1}, are

$$k_1(F) \cong \frac{k_D}{k_{-D}} k_1'(F) = K_D k_1'(F)$$

and (21)

$$k_{-1}(F) \cong k_{-1}'(F),$$

where K_D is the equilibrium constant for the diffusive part of the process. Thus the effective second-order rate constant, k_1, is approximately proportional to the calculated first-order rate constant, k_1'.

Force and the free energy of reaction

The results above also yield an expression for the standard free energy of reaction for

$$A \underset{k_f}{\overset{k_r}{\leftrightarrows}} B$$

as a function of force. At equilibrium the net probability current, J, must be zero, and

$$\frac{p_B}{p_A} = \frac{k_f}{k_r} = K_{eq} = e^{-\Delta G^0_{rxn}(F)/kT} = \frac{N_B}{N_A} = \frac{\int_\ell^L e^{-(V(s)+Fs)/kT} ds}{\int_0^\ell e^{-(V(s)+Fs)/kT} ds} \quad (22)$$

which yields

$$\Delta G^0_{rxn}(F) = -kT \ln\left(\frac{\int_\ell^L e^{-(V(s)+Fs)/kT} ds}{\int_0^\ell e^{-(V(s)+Fs)/kT} ds}\right) \quad (23)$$

If we take $\Delta G_{rxn} = \Delta G^0_{rxn} + kT \ln(p_B/p_A)$, then $\Delta G^0_{rxn}(F)$ is the free energy of reaction at load force F under conditions where species A and species B have equal populations.

Suppose that the potential, $V(s)$, has two wells separated by a barrier (Fig. 2 *a*), and let the wells be deep enough so that $e^{-V(s)/kT}$ is significant only in the neighborhood of the well bottoms. Suppose also that the well bottoms are of nearly identical shape, so that they differ only by a constant offset,

$$V(s)\big|_{\text{near bottom of well 1}} \cong V(s)\big|_{\text{near bottom of well 2}} + \Delta V_0,$$

where ΔV_0 is the constant energy difference from well 1 to well 2. Then the integrands in Eq. 23 are approximately δ-functions centered on the well bottoms, and the free energy reduces to

$$\Delta G^0_{rxn} \cong \Delta V_0 + Fx, \quad (24)$$

where x is the distance between the bottoms of the two wells. Thus the free energy is linear in F, as would be intuitively expected. Calculations using Eq. 23 show that if the wells are shallow or differ in shape, Eq. 24 is often still approximately correct, but the values of ΔV_0 and x no longer have the same simple physical interpretation. In other cases ΔG^0_{rxn} is not linear in force and Eq. 23 must be used. Fig. 2 *b* shows the calculated free energy of reaction for the same potential that was used to calculate the rate constants (a symmetric two-wells-with-barrier potential). The free energy is linear in force as expected from Eq. 24. Nonlinear free energies are easily obtained by varying well shape, however, especially if the wells are made unequal in size or shape. It is worth noting also that a linear free energy function does not imply an exponential form for the individual rate constants, though this has often been assumed. For example, in Fig. 2 *b* ΔG^0_{rxn} is linear even at very high and very low forces, where the rate constants are strongly nonexponential.

Stalling force

The stalling force for the motor, F_{stall}, is the value of F for which the motor velocity (and hence the current, J) is zero. Consider a reversible motor with only one force-dependent step. Then F_{stall} is the force needed to make the current through this step zero, which is the same as the force needed to make the free energy change zero. For cases where the free energy is linear in force,

$$\Delta G_{rxn} = \Delta V_0 + F_{stall} x + kT \ln(p_B/p_A) = 0,$$

which implies

$$F_{stall} = -\frac{\Delta V_0}{x} - \frac{kT}{x} \ln\left(\frac{p_B}{p_A}\right) \quad (25)$$

Thus the stalling force depends on both the driving free energy of the reaction, ΔV_0, and on the concentrations of reactants and products, p_A and p_B, as would be expected. Equation 25 predicts an infinite stalling force when p_B is zero. This reflects the fact that the chemical free energy, $\Delta G_{rxn} = \Delta G^0_{rxn} + kT \ln (p_B/p_A)$, also goes to infinity when p_B is zero. Physically, both the infinite stalling force and the infinite free energy arise from the fact that the motor cannot be reversed if the product concentration is zero. If the motor cannot step backward it will eventually step forward under the influence of thermal fluctuations, no matter how large the opposing force. For the same reason, any motor that has an irreversible step in an unbranched mechanism will have a formally infinite stalling force (and infinite free energy of reaction). (See, for example, the plots in Fig. 3, *a–c*). An infinite stalling force is clearly artificial: in any real system the walker will either walk backward by some slow kinetic path (at sufficiently long times), or the motor itself will deform (at sufficiently large forces). However, Eq. 25 suggests that the stalling force measured experimentally may not be easily compared quantitatively to a stalling force predicted theoretically. It also makes clear that the properties of a microscopic molecular motor subject to thermal

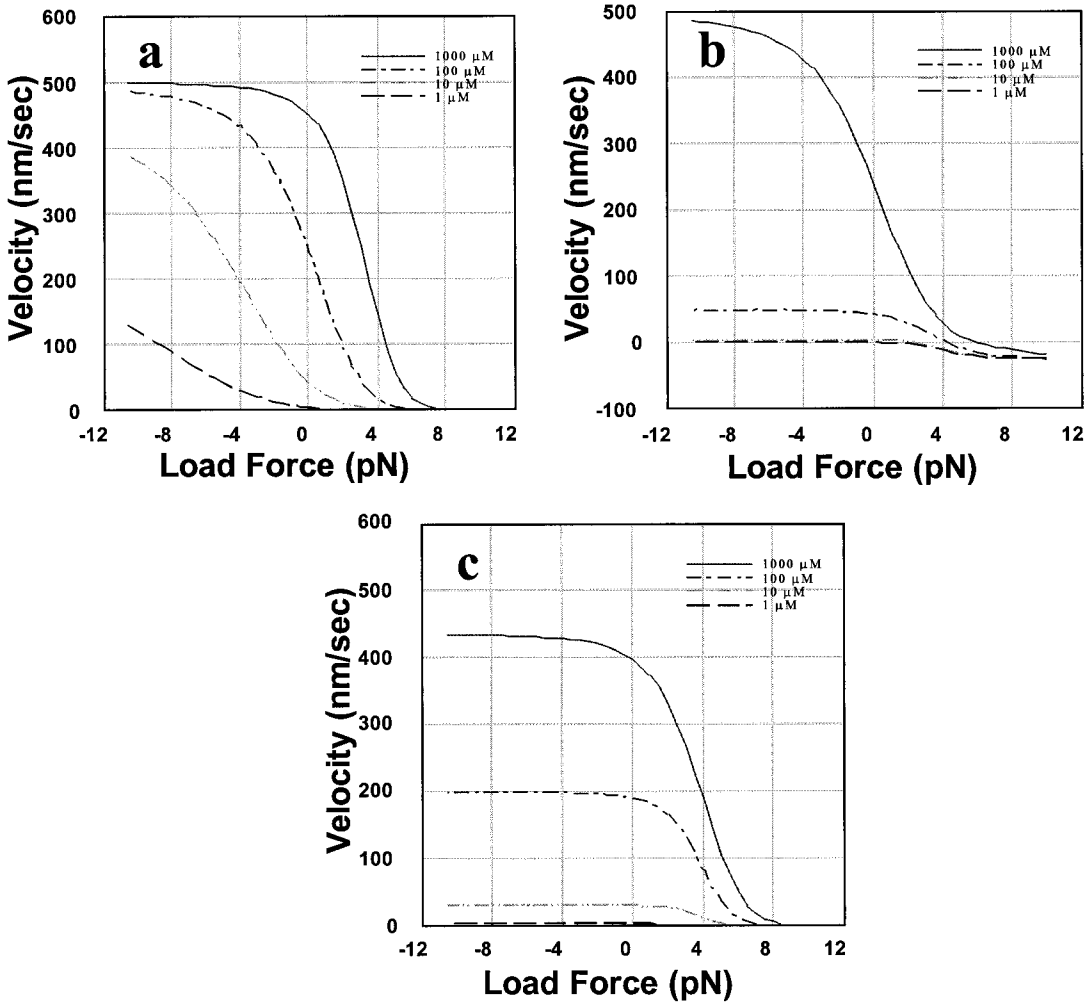

FIGURE 3 (*a*) Calculated force-velocity curves for the simplified mechanochemical binding mechanism at several ATP concentrations: $k_2 = 100\ s^{-1}$, $d = 5$ nm, and k_1 and k_{-1} calculated from the potential in Fig. 2 *a* with $\Delta V(0) = -12.5$, $\Delta V = 12.5$ kJ/mol, $\Delta V_0 = 12.5$ kJ/mol, $\Delta V(L) = 12.5$ kJ/mol, $\Delta s_f = 2.5$ nm, $\Delta s_r = 2.5$ nm, $\ell = 5$ nm, $L = 10$ nm, $\gamma = 4 \times 10^{-8}$ kg/s, $T = 300$ K. The K_D factor for k_1 was $1.07 \times 10^{-3}\ \mu M^{-1}$. (*b*) Calculated force-velocity curves for the simplified mechanochemical release mechanism with $k_1 = 1\ mM^{-1}\ s^{-1}$, $k_{-1} = 50\ s^{-1}$, and k_2 calculated using the same potential and parameters as in (*b*). (*c*) Calculated force-velocity curves for the simplified mechanochemical trigger mechanism with $k_1 = 1\ mM^{-1}\ s^{-1}$, $k_{-1} = 50\ s^{-1}$, $k_2 = 100\ s^{-1}$, and k_3 calculated using the same potential and parameters as in (*b*).

fluctuations can be very different from those of a similar motor with macroscopic dimensions.

EXAMPLE APPLICATIONS OF THE STOCHASTIC-KINETIC THEORY

The minimum experimental information needed to build a model

Using the results of the previous section it is possible to calculate the dynamical behavior of any molecular motor from knowledge of its potential energy surface. However, the potential energy surfaces of proteins are generally not known, and the best information available is usually a kinetic mechanism (i.e., a network of transitions between discrete species, as in Fig. 1 *c*) derived from macroscopic kinetics experiments. For transitions that do not involve net movement and hence do not depend on external force, the experimentally measured values of the rate constants can be used to describe motor dynamics directly; but for mechanochemical transitions, it is necessary to calculate how rate constants depend on force (e.g., using Eqs. 17, 18, and 20), and one-dimensional potentials along the local reaction coordinates, s, must be known (or estimated). Thus, the minimum information necessary to model the properties of a molecular motor is 1) the kinetic mechanism (with the corresponding rate constants) as determined by macroscopic kinetics, and 2) the identity of the mechanochemical steps together with some estimate of the one-dimensional potential energy curves for these steps.

Here we explore the general behavior to be expected from molecular motors. We do this by investigating four simple

yet general models that can be mapped onto a wide class of molecular motor mechanisms. The focus is on the steady-state motor velocity, v, as a function of external load force, F (the "force-velocity" curve), which is perhaps the most characteristic single-molecule measurement.

A minimal family of motor models

All kinetic mechanisms that describe a molecular motor, like all mechanisms that describe any enzyme, must be cyclic. That is, if the mechanism begins with a step in which a given state of the motor appears as a reactant, the same state of the motor must also appear as a product in some later step, and vice versa. The motor must bind fuel molecules, so its mechanism must contain at least one second-order step, and it must move and generate force, so at least one step must depend on external force. Virtually all proposed motor mechanisms also contain steps that are purely chemical and are not affected by force. To simplify matters, we consider only mechanisms with one force-dependent step, one fuel-binding step, and one product release step. Finally, the simplest kinetic mechanisms are unbranched, so that each intermediate state of the motor is connected to exactly two others in a (linear) kinetic mechanism. These restrictions define a limited class of models, shown schematically below:

Mechanochemical binding model

$$M_1 + T \underset{k_{-1}(F)}{\overset{k_1(F)}{\rightleftarrows}} M_2 \underset{k_{-2}}{\overset{k_2}{\rightleftarrows}} M_3 \underset{k_{-3}}{\overset{k_3}{\rightleftarrows}} M_4 + D \underset{k_{-4}}{\overset{k_4}{\rightleftarrows}} M_1$$

Mechanochemical reaction model

$$M_1 + T \underset{k_{-1}}{\overset{k_1}{\rightleftarrows}} M_2 \underset{k_{-2}(F)}{\overset{k_2(F)}{\rightleftarrows}} M_3 \underset{k_{-3}}{\overset{k_3}{\rightleftarrows}} M_4 + D \underset{k_{-4}}{\overset{k_4}{\rightleftarrows}} M_1$$

Mechanochemical release model

$$M_1 + T \underset{k_{-1}}{\overset{k_1}{\rightleftarrows}} M_2 \underset{k_{-2}}{\overset{k_2}{\rightleftarrows}} M_3 \underset{k_{-3}(F)}{\overset{k_3(F)}{\rightleftarrows}} M_4 + D \underset{k_{-4}}{\overset{k_4}{\rightleftarrows}} M_1$$

Mechanochemical trigger model

$$M_1 + T \underset{k_{-1}}{\overset{k_1}{\rightleftarrows}} M_2 \underset{k_{-2}}{\overset{k_2}{\rightleftarrows}} M_3 \underset{k_{-3}}{\overset{k_3}{\rightleftarrows}} M_4 + D \underset{k_{-4}(F)}{\overset{k_4(F)}{\rightleftarrows}} M_1$$

where M is the motor molecule, T is ATP (or another fuel molecule), D is ADP + P_i (or another set of products), and $k_i(F)$ indicates a force-dependent step.

This is the simplest group of motor models capable of describing a wide range of real motor behavior. Each model has four states in its mechanochemical cycle and four transitions between these states. The models differ only in the step that involves movement, and hence in which rate constants depend on force. In the first three cases movement (and force generation) coincides with some part of the ATP hydrolysis cycle (binding, reaction, or release), so movement is directly coupled to the chemical reaction. In the fourth case, the mechanochemical trigger mechanism, the hydrolysis cycle is independent of movement: external load does not affect the kinetic parameters of the catalytic part of cycle and substrate concentration does not affect the intrinsic velocity of the movement part of the cycle. The chemical energy is "stored" in the form of a strained state of the protein, M_4, and movement is then driven or "triggered" by release of the strain. The coupling between the mechanical and chemical events is thus indirect: the chemical and the mechanical steps of the motor are arranged sequentially in time, and a new set of catalytic steps cannot start if the previous cycle has not been completed.

All four mechanisms are tightly coupled in the sense that a single ATP hydrolysis must lead to a single movement step, and vice versa. However, any of these models can be made loosely coupled by adding branches that allow the movement step to be bypassed between hydrolysis cycles (many-to-one coupling), or allow the hydrolysis cycle to be bypassed between movements (one-to-many coupling).

Kinetics and velocity

The steady-state velocity per motor molecule, v, is the distance traveled in the movement step, d, multiplied by the net flux through the movement step, J_{move}: $v = dJ_{move}$. For example, in the mechanochemical binding model (case 1 above), for which movement occurs on the first step, the velocity is $v = d(k_1M_1 - k_{-1}M_2)$, where M_1 and M_2 are the steady-state concentrations (or populations) of the corresponding states of the motor. Equivalent expressions apply for the other three classes. The steady-state concentrations M_1, M_2, M_3, and M_4, are found by solving the appropriate kinetic equations. For any of the models above these are:

$$\begin{aligned}
\dot{M}_1 &= -(k_{-4} + k_1T)M_1 + k_{-1}M_2 + k_4M_4 = 0 \\
\dot{M}_2 &= k_1TM_1 - (k_{-1} + k_2)M_2 + k_{-2}M_3 = 0 \\
\dot{M}_3 &= k_2M_2 - (k_{-2} + k_3)M_3 + k_{-3}DM_4 = 0 \\
\dot{M}_4 &= k_{-4}M_1 + k_3M_3 - (k_{-3}D + k_4)M_4 = 0
\end{aligned} \tag{26}$$

with conservation condition $M_1 + M_2 + M_3 + M_4 = 1$. Solving these equations yields

$$v = d\left(\frac{aT - bD}{eT + fTD + gD + h}\right) \tag{27}$$

where d is the step size for the motor, T is ATP concentration, D is product (ADP and P_i) concentration, and

$$a = k_1k_2k_3k_4$$

$$b = k_{-1}k_{-2}k_{-3}k_{-4}$$

$$e = k_1(k_3k_4 + k_{-2}k_4 + k_2k_4 + k_2k_3) \tag{28}$$

$$f = k_1k_{-3}(k_{-2} + k_2)$$

$$g = k_{-3}(k_{-2}k_{-4} + k_2k_{-4} + k_{-1}k_{-4} + k_{-1}k_{-2})$$

$$h = k_2k_3k_4 + k_2k_3k_{-4} + k_{-1}k_3k_4 + k_{-1}k_3k_{-4} + k_{-1}k_{-2}k_4 + k_{-1}k_{-2}k_{-4}$$

Equations 27 and 28 hold for all four models. The only difference is that for the first model k_1 and k_{-1} depend on force, while for the second model k_2 and k_{-2} depend on force, etc.

In the limit of small product concentration ($D = 0$), step 3 is irreversible, and the velocity follows Michaelis-Menten kinetics in all cases:

$$v = d\left(V_{\max}\frac{T/K_M}{1 + T/K_M}\right) \tag{29}$$

with $V_{\max}$ and K_M given by

$$V_{\max} = \frac{a}{e} = \frac{k_2k_3k_4}{k_3k_4 + k_{-2}k_4 + k_2k_4 + k_2k_3}$$

$$K_M = \frac{h}{e} = \frac{k_2k_3k_4 + k_2k_3k_{-4} + k_{-1}k_3k_4 + k_{-1}k_3k_{-4} + k_{-1}k_{-2}k_4 + k_{-1}k_{-2}k_{-4}}{k_1(k_3k_4 + k_{-2}k_4 + k_2k_4 + k_2k_3)} \tag{30}$$

Classes of motor models

Many complex mechanisms can be reduced to one of the four cases above by combining several steps into a single, effective step, and redefining the rate constants appropriately. For example, a model in which two steps follow the hydrolysis cycle,

$$M_1 + T \underset{k_{-1}}{\overset{k_1}{\rightleftarrows}} M_2 \overset{k_3}{\rightarrow} M_3 \overset{k_3}{\rightarrow} M_4 + D \overset{k'_4}{\rightarrow} M_5 \overset{k'_5(F)}{\rightarrow} M_1$$

is equivalent to the mechanochemical trigger model (case 4 above) with $1/k_4 = 1/k'_4 + 1/k'_5(F)$. Similarly, many simpler models can be generated from one of the four cases by reducing the number of steps, or by making some steps irreversible. This amounts to setting the appropriate rate constants to zero or infinity in the mechanisms and formulas above (Eqs. 27–30). Thus each mechanism represents a large class of motor models rather than a single model. We believe that most real molecular motors fall into one of these four classes, or into a loosely coupled variant of them.

Calculated models

As examples of the models above, consider three simple special cases:

Simplified mechanochemical binding model

$$M + T \underset{k_{-1}(F)}{\overset{k_1(F)}{\rightleftarrows}} MT \overset{k_3}{\rightarrow} M + D$$

Simplified mechanochemical release model

$$M + T \underset{k_{-1}}{\overset{k_1}{\rightleftarrows}} MT \overset{k_2(F)}{\rightarrow} M + D$$

Simplified mechanochemical trigger model

$$M + T \underset{k_{-1}}{\overset{k_1}{\rightleftarrows}} MT \overset{k_2}{\rightarrow} M^* + D \overset{k_3(F)}{\rightarrow} M$$

The first model is a simplified version of the mechanochemical binding model above. It derives from the mechanochemical binding model by setting $k_4 = k_{-4} \rightarrow \infty$, and $k_2 = k_{-2} \rightarrow \infty$. This effectively makes species M_2 and M_3 into one combined species, MT, and also makes M_4 and M_1 into a combined species, M. With these choices Eqs. 30 reduce to $V_{\max} = k_3$, and $K_M = (k_3 + k_{-3})/k_1$. Similarly, the simplified mechanochemical release model and the simplified mechanochemical trigger model can be derived from the mechanochemical release model and the mechanochemical trigger model.

Because the release step is irreversible in all three models, all three obey Michaelis-Menten kinetics. However, for the simplified mechanochemical trigger mechanism it is possible to define a velocity for the catalytic part of the mechanism (i.e., the first two steps) alone:

$$v_{cat} = d\left(V^{cat}_{\max}\frac{T/K^{cat}_M}{1 + T/K^{cat}_M}\right) \tag{31}$$

with $V^{cat}_{\max} = k_3$ and $K^{cat}_M = (k_{-1} + k_3)/k_1$. These "purely catalytic" Michaelis-Menten parameters are independent of force, consistent with the separation of chemistry and mechanics in the mechanochemical trigger model. In terms of v_{cat}, the velocity of the simplified mechanochemical trigger model is given by

$$\frac{1}{v} = \frac{1}{v_{cat}} + \frac{1}{v_{mov}} \tag{32}$$

where $v_{mov} = k_4d$. Equation 32 is just a statement that for the simplified mechanochemical trigger model, with its independent catalytic and movement processes, the total time required to complete a cycle, d/v, is the sum of the times for catalysis, d/v_{cat}, and for movement, d/v_{mov}.

Calculations

To calculate the force-dependent rate constants in the three models above, a piecewise-linear, two-wells-with-barrier potential was used (Fig. 2 *a*: barrier height $\Delta V = 12.5$ kJ/mol ($\sim 5\ kT$ at 300 K), reaction free energy $\Delta V_0 = 12.5$ kJ/mol, and well separation, $d = 5$ nm). For the simplified

mechanochemical binding mechanism, the value of K_D in the second-order rate constant, $k_1 = K_D k_1'$, was chosen so that $k_1 = 1\ \mu M^{-1}\ s^{-1}$ at zero force (Ma and Taylor, 1997). Equations 20 were then used to calculate the force-dependent rate constants, and Eqs. 29 and 30 were used to calculate the velocity. The results for all three models are shown in Fig. 3, *a–c,* for several ATP concentrations. Several features are noteworthy:

1. In all cases the velocity decreases monotonically with increasing load, but in many of the curves the velocity is almost independent of load force over a wide range. This is also a common feature in experimentally measured force-velocity curves (Wang et al., 1998b; Coppin et al., 1997), and results whenever the rate-limiting step for the motor is not force-dependent. The forward rate constant for any force-dependent step always decreases with increasing load, but this has no effect on the velocity unless the rate constant is similar to or smaller than the rate constant of the slowest force-independent step. In the examples shown, the velocity begins to drop at negative load for some curves, but it is possible (by lowering the potential barrier, ΔV, or increasing the driving free energy, ΔV_0) to make the constant region extend to positive forces, nearly up to the apparent stalling force.
2. In Fig. 3, *a* and *c,* the velocity is roughly linear at intermediate loads (e.g., 3–4 pN for the 1000 μM curve of Fig. 3 *a*) and then decays exponentially at very high loads (near apparent stall). This asymptotic drop to zero is a consequence of the irreversible second step in the simplified mechanisms, which does not allow the motor to be pushed backward (and hence does not allow negative velocity), even under infinite load. As mentioned above, any irreversible motor has a formally infinite stalling force. All real motors must be reversible (at least slowly), and the stalling force must therefore be finite, but the true stalling force may be difficult to measure experimentally. For example, the apparent stalling force (where the velocity becomes "very small") of the mechanochemical binding motor in Fig. 3 *a* seems to be finite and to depend on ATP concentration, but the theoretical stalling force is infinite, independent of concentration.
3. An example of a (weakly) reversible motor is shown in Fig. 3 *b,* the simplified mechanochemical release model. As written above, the mechanochemical release model is not reversible because it has no back-reaction at step 2; that is, the reverse rate constant, k_{-2}, is zero. However, k_{-2} is a force-dependent rate constant in this model, and in the actual calculations it becomes significant at high load, resulting in small negative velocities. For reversible models the crossover from positive to negative velocity unambiguously defines the stalling force. By adjusting the values of the rate constants or the parameters of the potential energy function, it is possible to make models that are easily and fully reversible.
4. As the ATP concentration decreases, the velocity decreases at all forces. For the mechanochemical binding model the force dependent rate constant, k_1, is second-order, so at high positive load, where the curves closely follow $k_1 T$, the concentration essentially multiplies the curve without changing the maximum velocity that is achieved at large negative load. For the mechanochemical release model the (second-order) binding step becomes rate-limiting at large negative force, where the (force-dependent) release step is large. Thus, the maximum velocity is roughly proportional to T, and achieves very large values at high ATP concentration. The mechanochemical trigger model depends on concentration only through the catalytic velocity, v_{cat}. At large negative load, where the mechanical velocity, $v_{mov} = k_4 d$, is large, the time required for the movement step is negligible, and the observed velocity becomes identical to the catalytic velocity, $v = v_{cat} d$. The limiting velocity at large negative load therefore varies with concentration according to Michaelis-Menten kinetics with K_M and V_{max} from the catalytic part.

Classifying motors from experimental data

The general expressions above are quite complex, but some aspects of their behavior can be understood qualitatively in a simple way. This understanding can, in turn, be used to help determine which (if any) of the models above are consistent with experimental force-velocity data for particular motors. First, according to the results above, all four models obey Michaelis-Menten kinetics when the product concentration, D, is zero. For a Michaelis-Menten motor, a plot of inverse velocity versus inverse ATP concentration is a straight line:

$$\frac{1}{v} = \frac{1}{d}\left(\frac{1}{V_{max}} + \frac{K_M}{V_{max}}\frac{1}{T}\right) \tag{33}$$

The slope of the line is $K_M/(dV_{max})$ and the intercept is $1/(dV_{max})$. Because the rate constants depend on force, the values of V_{max} and K_M also depend on force in general, and hence so do the slope and intercept. In special cases, how-

TABLE 1 Behavior of inverse plots for

$$M_1 + T \underset{-1}{\overset{1}{\rightleftarrows}} M_2 \overset{2}{\rightarrow} M_3 \overset{3}{\rightarrow} M_4 + D \overset{4}{\rightarrow} M_1$$

Movement Step	Intercept $1/(dV_{max})$	Slope $K_M/(dV_{max})$	K_M
Step 1 (binding)	Force-Independent	Force-Dependent	Force-Dependent
Step 2	Force-Dependent	Force-Dependent	Force-Dependent
Step 3 (release)	Force-Dependent	Force-Independent	Force-Dependent
Step 4	Force-Dependent	Force-Independent	Force-Dependent

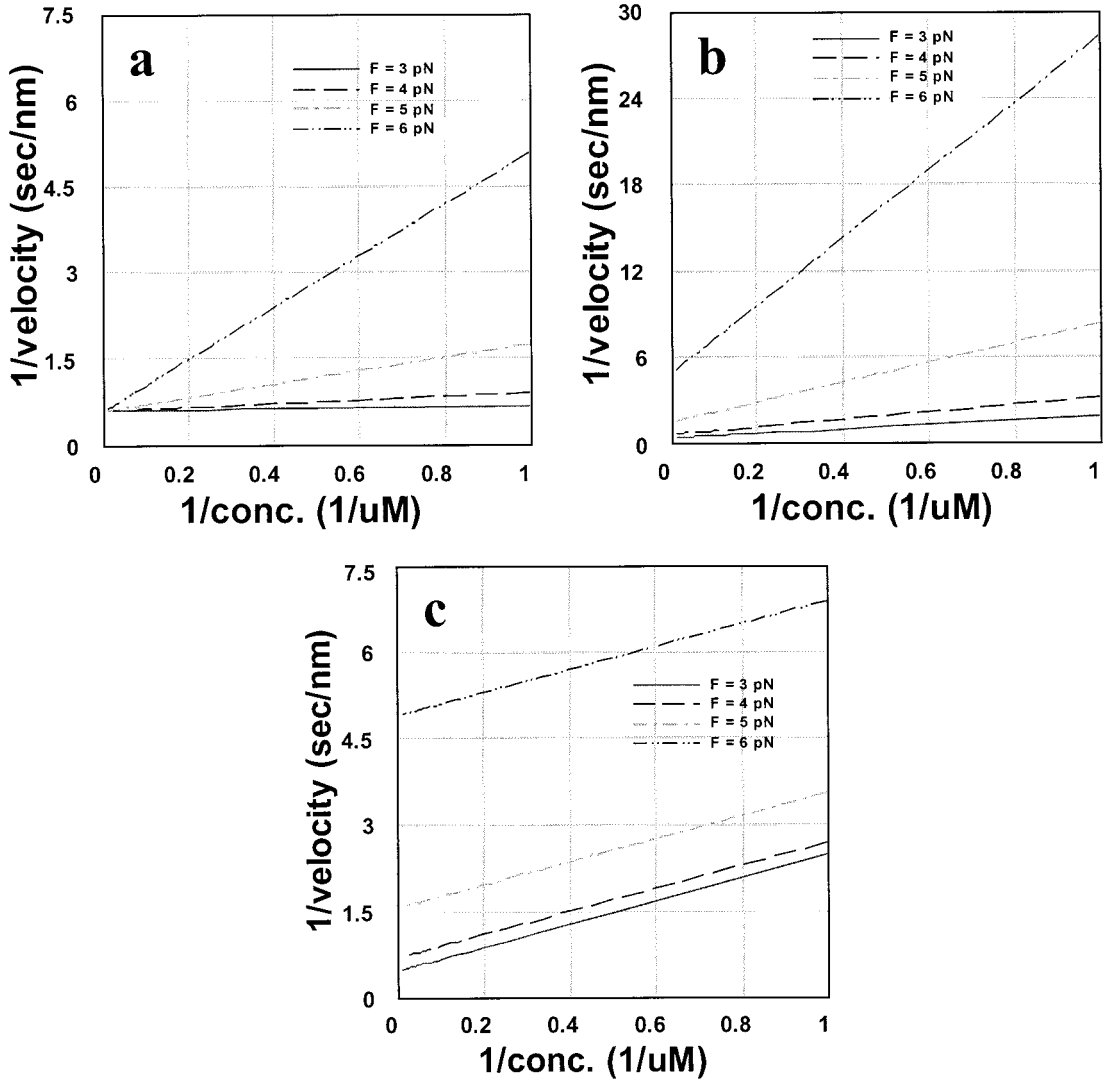

FIGURE 4 (*a*) Calculated inverse velocity versus inverse ATP concentration at several forces, for the case where the ATP binding step depends on external force. The force-dependent rate constants k_1 and k_{-1} were calculated from the potential in Fig. 2 *a,* with the same parameters as for the calculations in Fig. 3 *a,* and $K_D = 1.0\ \mu M^{-1}$. The rate constants for the force-independent steps were $k_2 = k_3 = k_4 = 1.0\ s^{-1}$. (*b*) Inverse velocity versus inverse ATP concentration for the case where step 2 depends on force. The force-dependent rate constants k_2 and k_{-2} were calculated as in (*a*). For this potential the reverse rate constant, k_{-2}, is small at these load forces. The rate constants for the force-independent steps were $k_1 = 0.2\ \mu M^{-1}\ s^{-1}$, $k_{-1} = k_3 = k_4 = 1.0\ s^{-1}$. (*c*) Inverse velocity versus inverse ATP concentration for the case where step 3 or 4 depends on force. The force-dependent rate constants k_3 and k_{-3} (or k_4 and k_{-4}) were calculated as in (*a*). The rate constants for the force-independent steps were $k_1 = 0.2\ \mu M^{-1}\ s^{-1}$, $k_{-1} = k_2 = k_{3\text{ or }4} = 1.0\ s^{-1}$.

ever, either slope or intercept may be independent of force. For example, suppose that solution kinetic measurements for a particular motor are consistent with a mechanism with a reversible binding step and three irreversible steps:

$$M_1 + T \underset{k_{-1}}{\overset{k_1}{\rightleftarrows}} M_2 \overset{k_2}{\rightarrow} M_3 \overset{k_3}{\rightarrow} M_4 + D \overset{k_4}{\rightarrow} M_1$$

Because this mechanism is based on solution kinetics, the step where movement takes place is not known. Because steps 2–4 are irreversible, $k_{-2} = k_{-3} = k_{-4} = 0$, and V_{max}, K_M, and K_M/V_{max} reduce to

$$V_{max} = \frac{a}{e} = \frac{k_2k_3k_4}{k_3k_4 + k_2k_4 + k_2k_3}$$

$$K_M = \frac{h}{e} = \frac{k_2k_3k_4 + k_{-1}k_3k_4}{k_1(k_3k_4 + k_2k_4 + k_2k_3)} \qquad (34)$$

$$\frac{K_M}{V_{max}} = \frac{h}{a} = \frac{k_2 + k_{-1}}{k_1k_2}$$

Thus V_{max} is independent of k_1 and k_{-1}, and K_M/V_{max} is independent of k_3, k_{-3}, k_4, and k_{-4}. Therefore, if step 1 (the

binding step) involves movement, and if the mechanism deduced from solution kinetics is correct, it will be found that the motor obeys Michaelis-Menten kinetics, and that in plots of $1/v$ vs. $1/T$ the intercept is independent of force, but the slope varies. However, if movement occurs on steps 3 or 4 the slope will be independent of force, but the intercept will vary. Finally, if the movement occurs on step 2, both slope and intercept will vary with force. Thus three of the four possible positions for the movement step can be distinguished from the qualitative behavior of the inverse plots alone. Table 1 summarizes these results, and Fig. 4 shows an example of $1/v$ vs. $1/T$ plots for the three distinguishable cases. A similar analysis can be carried out with any model that belongs to one of the four classes above. Once the movement step has been determined, a well-founded model for how the corresponding rate constants depend on force can be constructed using the theory in the first section. Force-velocity curves may then be calculated from Eqs. 27–30 and directly compared to experimental force-velocity curves.

SUMMARY AND CONCLUSIONS

The theory described above embodies the basic physics of mechanochemistry. The theory is simple enough to be applied to large, complex systems where structural information is limited, yet general enough to apply to any motor. The main approximations of the theory—that the system behaves classically, that the time scale of the experiments is long compared to the microscopic fluctuations, and that individual steps can be described by one-dimensional reaction coordinates—are likely to be very good for most molecular motors. It is therefore possible to go from the detailed, microscopic picture to the coarser, macroscopic, kinetic picture in a consistent way. Most of the difficulties and details in dealing with a protein are hidden in the phenomenological rate constants, and most of these are taken from experiment. Only the relatively few steps that depend on force need be treated theoretically.

The minimum information required to make a complete model is 1) the values of the kinetic rate constants for nonmechanical processes, and 2) estimates of the shape of the one-dimensional potential energy function, $V(s)$, for mechanical steps. In calculations we find that the rate constants are mainly sensitive to a few properties of the potential: the energy differences from potential well bottoms to the barrier top and the distances from the well bottoms to the position of the barrier maximum. Thus, a complete theory for a molecular motor depends on a relatively small number of phenomenological parameters. Many of the structural and mechanistic assumptions used in models that have appeared in the literature for particular molecular motors are essentially methods for estimating rate constants and the shapes of potential energy functions (Peskin and Oster, 1995; Wang et al., 1998a).

Designed motors?

From the theory above it is clear that any enzyme for which catalysis involves a (large) conformational change can act as a motor. Whenever movement accompanies a chemical step, the protein is inherently mechanochemical. For example, hexokinase is a soluble enzyme from the glycolysis pathway that ordinarily has no mechanical function. But when it binds glucose and ATP, a large cleft closes and two domains move relative to each other by up to 8 Å (Voet and Voet, 1995). Because of this large movement, hexokinase couples chemical energy to forces and motion. Therefore, if a hexokinase molecule (or perhaps a long chain of molecules) were linked between two points, it would generate tension and net contraction during its catalytic cycle. In such an experiment the kinetic and thermodynamic properties of hexokinase would be affected by an external load in the same way as a true molecular motor. Mechanochemical theory and single-molecule mechanical measurements can therefore be used to understand the function and mechanisms of a wide variety of enzymes.

References

Astumian, R. D. 1997. Thermodynamics and kinetics of a Brownian motor. *Science.* 276:917–922.

Astumian, R. D., and M. Bier. 1994. Fluctuation-driven ratchets: molecular motors. *Phys. Rev. Lett.* 72:1766–1769.

Astumian, R. D., and M. Bier. 1996. Mechanochemical coupling of the motion of molecular motors to ATP hydrolysis. *Biophys. J.* 70:637–653.

Chandrasekhar, S. 1943. Stochastic problems in physics and astronomy. *Rev. Mod. Phys.* 15:1–89.

Coppin, C. M., J. T. Finer, J. A. Spudich, and R. D. Vale. 1996. Detection of sub-8-nm movements of kinesin by high-resolution optical-trap microscopy. *Proc. Natl. Acad. Sci. USA.* 93:1913–1917.

Coppin, C. M., D. W. Pierce, L. Hsu, and R. D. Vale. 1997. The load dependence of kinesin's mechanical cycle. *Proc. Natl. Acad. Sci. USA.* 94:8539–8544.

Derenyi, I., and T. Vicsek. 1996. The kinesin walk: a dynamic model with elastically coupled heads. *Proc. Natl. Acad. Sci. USA.* 93:6775–6779.

Derenyi, I., and T. Vicsek. 1998. Realistic models of biological motion. *Physica A.* 249:397–406.

Elston, T., H. Wang, and G. Oster. 1998. Energy transduction in ATP synthase. *Nature.* 391:510–513.

Finer, J. T., R. B. Simmons, and J. A. Spudich. 1994. Single myosin molecule mechanics: piconewton forces and nanometer steps. *Nature.* 368:113–119.

Guajardo, R., and R. Sosa. 1997. A model for the mechanism of polymerase translocation. *J. Mol. Biol.* 265:8–19.

Higuchi, H., E. Muto, Y. Inoue, and T. Yanagida. 1997. Kinetics of force generation by single kinesin molecules activated by laser photolysis of caged ATP. *Proc. Natl. Acad. Sci. USA.* 94:4395–4400.

Hua, W., E. C. Young, M. L. Fleming, and J. Gelles. 1997. Coupling of kinesin steps to ATP hydrolysis. *Nature.* 388:390–393.

Julicher, F., A. Ajdari, and J. Prost. 1997. Modeling molecular motors. *Rev. Mod. Phys.* 69:1269–1281.

Julicher, F., and R. Bruinsma. 1998. Motion of RNA polymerase along DNA: a stochastic model. *Biophys. J.* 74:1169–1185.

Kubo, R., M. Toda, and N. Hashitsume. 1995. Statistical Physics II: Nonequilibrium Statistical Mechanics, 2nd ed. Springer, Heidelberg.

Kuo, S. C., and M. P. Sheetz. 1993. Force of single kinesin molecules measured with optical tweezers. *Science.* 260:32–34.

Ma, Y.-Z., and E. W. Taylor. 1997. Interacting head mechanism of microtubule-kinesin ATPase. *J. Biol. Chem.* 272:724–730.

Magnasco, M. O. 1994. Molecular combustion motors. *Phys. Rev. Lett.* 72:2656–2659.

Magnasco, M. O. 1993. Forced thermal ratchets. *Phys. Rev. Lett.* 71: 1477–1481.

McQuarrie, D. A. 1976. Statistical Mechanics. Harper & Row, New York. 266.

Mehta, A. D., J. T. Finer, and J. A. Spudich. 1997. Detection of single-molecule interactions using correlated thermal diffusion. *Proc. Natl. Acad. Sci. USA.* 94:7927–7931.

Millonas, M. M. 1995. Self-consistent theory of fluctuation-induced transport. *Phys. Rev. Lett.* 74:10–13.

Millonas, M. M., and M. I. Dykman. 1994. Transport and current reversal in stochastically driven ratchets. *Phys. Lett. A.* 185:65–69.

Mori, H. 1965. Transport, collective motion, and Brownian motion. *Prog. Theor. Phys.* 33:423–455.

Peskin, C. S., and G. Oster. 1995. Coordinated hydrolysis explains the mechanical behavior of kinesin. *Biophys. J.* 68(Suppl.):202–211.

Schnitzer, M. J., and S. M. Block. 1997. Kinesin hydrolyzes one ATP per 8-nm step. *Nature.* 388:387–389.

Spudich, J. A. 1994. How molecular motors work. *Nature.* 372:515–518.

Svoboda, K., C. F. Schmidt, B. J. Schnapp, and S. M. Block. 1993. Direct observation of kinesin stepping by optical trapping interferometry. *Nature.* 365:721–727.

Voet, D., and J. Voet. 1995. Biochemistry, 2nd ed. J. Wiley & Sons, New York. 447.

Vugmeyster, Y., E. Berliner, and J. Gelles. 1998. Release of isolated single kinesin molecules from microtubules. *Biochemistry.* 37:747–757.

Wang, H-Y, T. Elston, A. Mogliner, and G. Oster. 1998a. Force generation in RNA polymerase. *Biophys. J.* 74:1186–1202.

Wang, M. D., M. J. Schnitzer, H. Yin, R. Landick, J. Gelles, and S. M. Block. 1998b. Force and velocity measured for single molecules of RNA polymerase. *Science.* 282:902–907.

Yin, H., M. D. Wang, K. Svoboda, R. Landick, S. M. Block, and J. Gelles. 1995. Transcription against an applied force. *Science.* 270:1653–1657.